Procds. of the 16th Asian Regional Conference on Soil Mechanics and Geotechnical Engineering,
October 14-18, 2019, Taipei, Taiwan

Application of 3D LiDAR technology in adjacent construction of triple tunnel

Kwojane Kuo[1], T. Chu[2], C. Huang[2], H. Tseng[1], T. Tseng[3]

[1] T.Y.Lin Taiwan Consulting Engineers, Inc., Taipei, Taiwan
[2] Public Work Department, New Taipei Government, Taipei, Taiwan
3 Chune-Hsing Surveying Co., Taipei, Taiwan

ABSTRACT

3D LiDAR scanning monitoring technology can quickly scan the object. It has high-density and high-precision scanning object's three-dimensional spatial data characteristics without reflection prism. At present, Ground-based laser scanner has been widely used in the sliding collapse of hillside slopes, highway bridges, and tunnel for deformation monitoring purpose, i.e., MRT tunnels and hydraulic engineering tunnels. If a new tunnel project is built in a relatively young geological age or in a deformation-oriented stratum, surrounding rock disturbance caused by tunnel excavation may affect the safety of neighboring areas and construction workers. Traditional tunnel convergence deformation measurement cannot fully reflect the full impact of tunnel excavation disturbance. It is also impossible to fully control the deformation behavior mode of rock mass after excavation. This paper presents a comprehensive monitoring study of an adjacent excavation and shallow-covered tunnel consisting of a three-arch tunnel in the Xindian area of northern Taiwan. The displacement of the surrounding rock of the tunnel is reduced due to the effective application of the central RC wall. The paper aims to explain the application of the optical scanning monitoring results, to provide the overall circular displacement trend of the tunnel and the equivalent displacement contour map along the tunnel, which can provide accurate tunnel safety monitoring, and establish a new thinking on tunnel safety monitoring for adjacent construction of tunnel. The 3D LiDAR scanning monitoring results can be effectively applied in subsequent similar cases.
Keywords: Ground-based LiDAR, adjacent excavation, shallow-covered tunnel, three-arch tunnel

1 INTRODUCTION

Building a new highway tunnel in the metropolitan area is generally limited to the dense residential and the area of land acquirement. The twin tunnels with excavation diameter of 13m are built in the Xindian area of northern Taiwan. These tunnels aim to satisfy the traffic capacity of one-way double lane road. Due to traffic network planning, a light rail MRT tunnel with excavation diameter of 12m must be set up between the two road tunnels. Because the land use is limited, the spacing between each tunnel is only about 1.5m. The geological material is very weak in strength and the central pillar of rock cannot support the overlying rock pressure after the tunnel is excavated. Therefore, it is proposed to use the small-section central pilot method (height × width = 6m × 6.5m) for excavation. This five-arched tunnel is the first case in Taiwan (Fig. 1). Each pilot constructed by RC wall (1.5m wide) provides sufficient compression and shear strength to reduce tunnel excavation deformation.

The multi-arch tunnel has shallow coverage, weak strength of the rock mass material, and multiple adjacent tunnel construction characteristics. The rock mass may be disturbed after each sequential tunnel excavation and it may affect adjacent completed tunnels. After the excavation and support of tunnel, surrounding rock displacement behavior may not accurately be predicted by traditional two-dimensional monitoring method. In this case, the high-precision three-dimensional coordinates of the surrounding rock of the adjacent tunnel are obtained by the 3D LiDAR (also known as ground-based LiDAR) which can comprehensively monitor the deformation behavior of rock mass after tunnel excavation.

Fig. 1. Multi-arched tunnels in Taipei, ROC.

2 PROJECT INFORMATION

The project case is located in the Xindian area in northern Taiwan. The tunnel configuration plan is shown in Fig. 2. The longitudinal and transverse sections of the triple tunnel and the distribution of rock cover height are shown in Fig. 3 and 4.

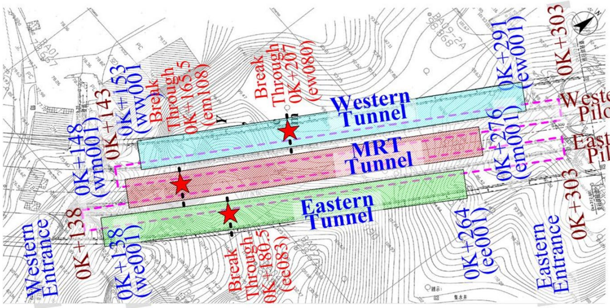

Fig. 2. Tunnel configuration layout.

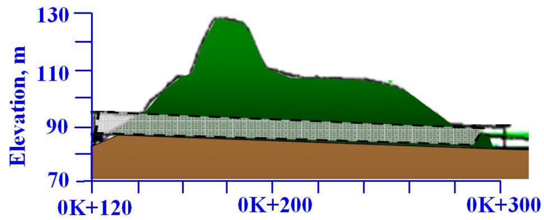

Fig. 3. Tunnel longitudinal section.

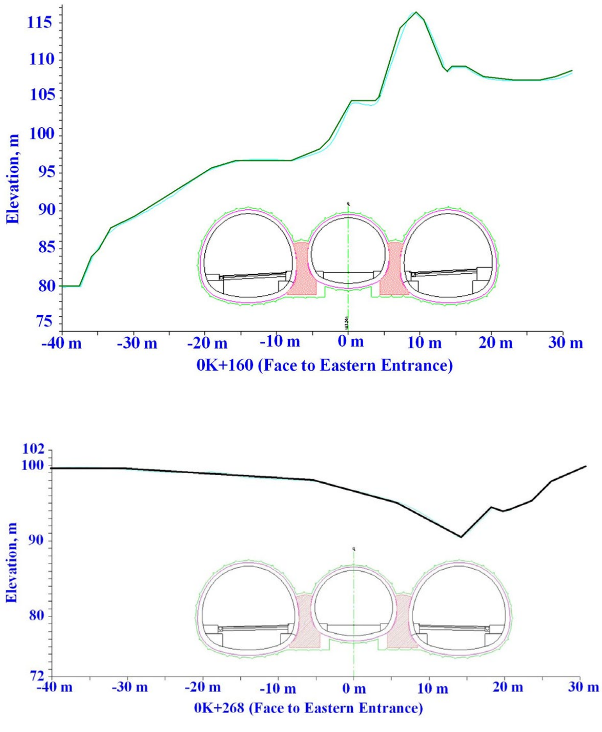

Fig. 4. Tunnel transverse profile (0K+160, 0K+268).

2.1 Tunnel Excavation Sequence

The pilot between tunnels that composed by RC wall will be constructed before the tunnel excavation. Each tunnel will be divided into 3 stages of excavation. After the completion of the central pilot (western and eastern pilot), the first excavation phase starts at the middle tunnel (MRT Tunnel) and continues for the eastern and western tunnel. The cross-sectional configuration of the tunnel is shown in Fig. 5. The tunnel is excavated from the east and west entrances to the middle of the tunnel. As ssown in Fig.2, the symbol ‘em001’ in the figure indicates the excavation sequence position, the first letter ‘e’ indicates excavation from the eastern entrance, the second letter ‘m’ indicates the MRT tunnel, and the number ‘001’ indicates the first ring of tunnel excavation. If the first letter is ‘w’, it means excavation starts from the western entrance. If the second letter is ‘e’ or ‘w’ it means the eastern tunnel and the western tunnel, respectively. The detailed construction period of each tunnel is described in Table 1.

Table 1. Summary of construction period for all tunnels

Construction Item	Eastern Entrance	Western Entrance
Eastern Pilot	0K+303~148 (2016/12/13~2017/04/16)	0K+134~148 (2017/03/04~2017/04/16)
Western Pilot	0K+303~167 (2017/01/16~2017/05/23)	0K+143~167 (2017/05/23~2017/05/23)
Eastern Pilot RC wall	2017/07/02~2017/08/19(From East to West)	
Western Pilot RC wall	2017/09/23~2018/02/07(From East to West)	
MRT Tunnel	0K+276~165.5 (2017/11/24~2018/03/18)	0K+148~165.5 (2018/03/04~2018/03/18)
Eastern Tunnel	0K+264~180.5 (2018/04/01~2018/06/15)	0K+138~180.5 (2018/04/18~2018/06/15)
Western Tunnel	0K+291~207 (2018/06/15~2018/09/05)	0K+153~207 (2018/06/18~2018/09/05)

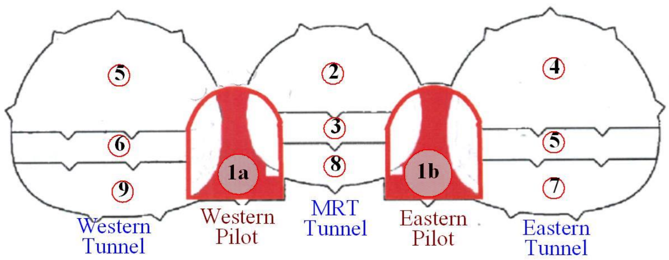

Fig. 5. Cross-section configuration with multi-arch of tunnel and tunnel excavation sequence.

2.2 Regional Geology and Terrains

The Xindian area is a mountainous terrain, the rock mass is generally weak and deformable due to weathering factor. The geological materials in the scope of this project belong to the Nanzhuang Formation without geological structures passed. The rock mass is weakly cemented and classified to extremely weak rock. Since the geologic structural weak surface is not developed, the rock mass is regarded as a homogeneous isotropic material. The average rock compressive strength is 30kg/cm^2 in the mileage of 0K+140~220, meanwhile in the mileage of 0K+200~300 the average of rock compressive strength is $3kg/cm^2$. Generally, the rock strength is higher on the east side and becomes lower on the west side.

3 3D LIDAR SCANNING AND MONITORING TECHNOLOGY

3D LiDAR scanning technology has sprouted since the 1970s. It is originally developed by NASA of the US Aerospace Department. The 3D LiDAR scanner is a new measurement tool that can scan the object quickly and acquire comprehensive spatial 3D information. It can directly obtain a high-density and high-precision three-dimensional space without reflection prism required and having a relative coordinate system for the surveying data (Fig. 6).

Fig. 6. 3D LiDAR scanning schematic and spatial three-dimensional information.

4 SCAN MONITORING TECHNOLOGY RESULTS

4.1 3D LiDAR scanning and monitoring results

3D LiDAR scanning technology can provide full-section displacement monitoring results of tunnel under adjacent excavation. It can obtain the surrounding rock displacement and control the possible stress behavior caused by excavation of the rock around the adjacent tunnel. To replace the traditional prism type of internal space displacement with inadequacy of measurement data. It can be more accurate and comprehensive in controlling the displacement changes in the surrounding rock of the tunnel. The differential monitoring displacement between the 3D LiDAR and traditional method is shown in Fig. 7.

The point cloud data obtained by the 3D LiDAR scanning can be obtained by multi-stage overlapping data procedure. By these procedures, the coordinate and displacement change of the same position can be obtained as shown in Fig. 6. Fig. 8 shows the equivalent displacement contour of the eastern pilot. The contour shows that the X axis is the tunnel mileage distance, the Y axis is an expanded view from the left to right side walls of the tunnel section (based on facing to eastern entrance).

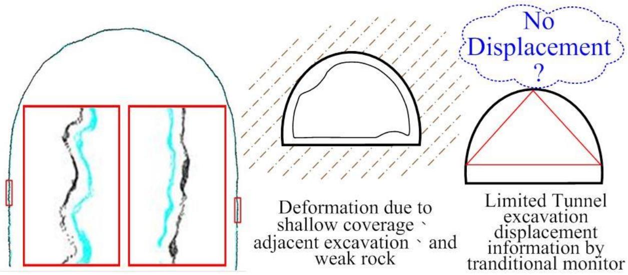

Fig. 7. Difference between full-section and traditional monitoring.

Different colors in the contour indicate the change of displacement after tunnel excavation. Also, it can be supplemented with a scan result image to initially assess the abnormal change.

Fig. 8 shows the larger surrounding rock displacement of monitoring results located at upper and lower of the contour for full face cut in eastern pilot (i.e., left and right tunnel side walls). The arch of the tunnel using pipe umbrella roofing method plays a better supporting effect, therefore there is no significant deformation in the side wall. The arch of the tunnel is expanding affected by the extrusion of the left and right side walls at some areas of the tunnel (blue and purple color in the contour). In addition, it is noticeable at the eastern entrance (0K+260~300) and western entrance (0K+140~160) there are a large displacement affected by the shallow coverage and the unsymmetrical load on tunnel after the tunnel is excavated.

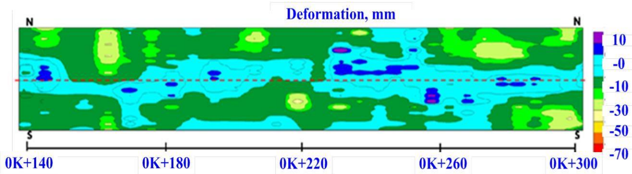

Fig. 8. Equivalent displacement contour of the eastern pilot.

4.2 Tunnel Duration Curve

The deformation data of the tunnel excavation is arranged, and Fig. 9 shows the duration curve of the eastern and western pilot. Overall, the maximum displacement δ_{max} is 29mm, 38mm, and 16mm for eastern entrance, western entrance, and intermediate section, respectively. And the displacement at the eastern pilot is slightly larger than the western pilot within a range 1.9~3.3mm.

Fig. 10 shows the MRT tunnel duration curve. Since the MRT tunnel is excavated after the construction of the eastern and western central RC wall is completed, the maximum displacement δ_{max} is only 6 mm in two months after this tunnel breaks through on 2018/03/18. It is obvious that the central RC wall plays a role in reducing the displacement of the rock mass. Afterwards, there is keeping displacement due to the construction of adjacent tunnels. At initial stage, the maximum displacement caused by the eastern tunnel construction is up to 10~15mm, then the maximum displacement caused by the western tunnel construction is up to 20~25mm.

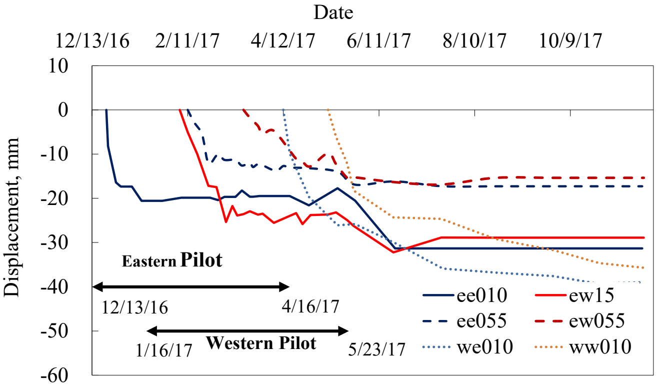

Fig. 9. The duration curve of eastern and western pilot (East, middle, and west).

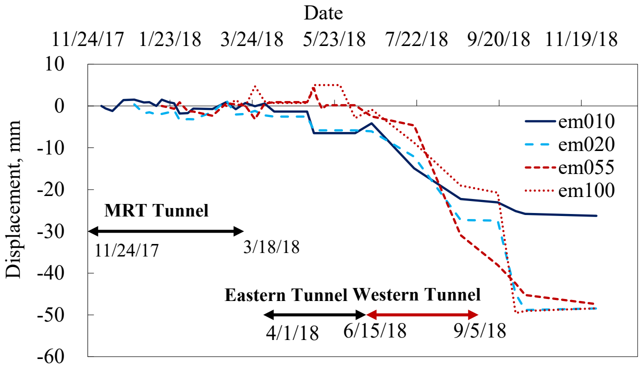

Fig. 10. The duration curve of MRT pilot (East, middle, and west).

Fig. 11 shows the duration curve of the eastern tunnel. The MRT tunnel has been excavated through during the construction of the eastern tunnel, thus it is less affected by the MRT tunnel. The maximum displacement δ_{max} is only 9.5mm in 1.5 months after this tunnel breaking through on 2018/06/15, and the maximum displacement δ_{max} gradually increases from 13mm to 40mm caused by the subsequent rainfall events and the western tunnel construction. The terrain ridgeline is also a factor that weakened rock strength due to rainfall the main affected road section is between 0K+168 to 264.

Fig. 12 shows the duration curve of the western tunnel. The MRT and eastern tunnel have been bored through during the construction of the western tunnel. In addition, the construction period was in the rainy season. Overall, the maximum displacement δ_{max} is 19.5mm, 29.6mm, and 16mm for eastern entrance, western entrance, and intermediate section, respectively. And the increment displacement $\Delta\delta_{max}$ of the tunnel rock mass is increased within 10~15mm due to rainfall.

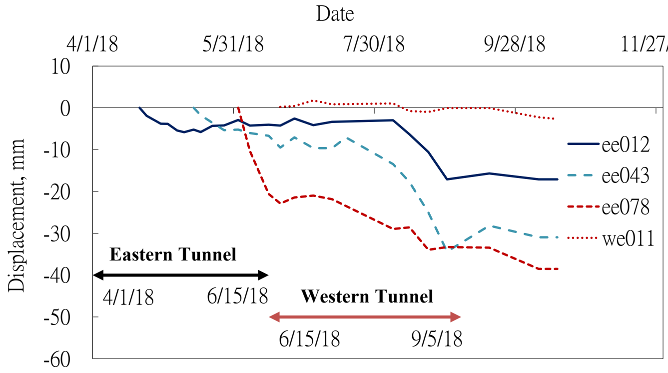

Fig. 11.The duration curve of Eastern tunnel (East, middle, and west).

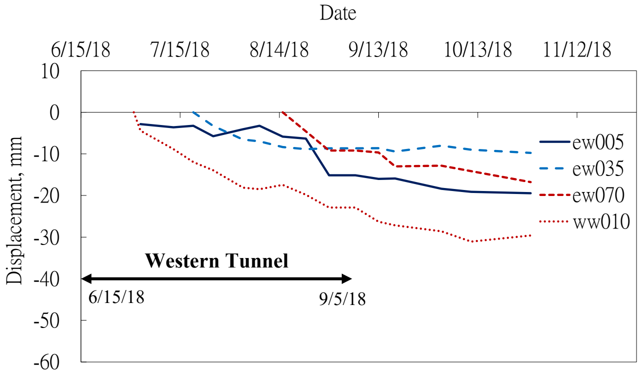

Fig. 12.The duration curve of Western tunnel (East, middle, and west).

4.3 Tunnel Surrounding Rock Radial Displacement

To organize the deformation data of the tunnel excavation, Fig. 13 shows the radial displacement of the surrounding rock at the eastern entrance, western entrances, and the middle section of the eastern and western pilot (facing to eastern entrance). On the whole, the terrain in eastern entrance is a valley, thus the displacement is affected by the unsymmetrical load above the tunnel. As the result, the southern side wall of the eastern tunnel has larger deformation, but the northern side wall of the wester tunnel has larger deformation. The middle section is less affected by the terrain behavior due to the unsymmetrical load above tunnel. Because of the terrain of western entrance is higher in the south and lower in the west, thus the displacement is also affected by the unsymmetrical load above tunnel.

The full-section displacement monitoring results of the tunnel provided by the 3D LiDAR scanning technology can obtain the displacement of the tunnel in all directions. It contribute to the reasonable assessment for the deformation behavior. The overall terrain is characterized by higher rock cover on the south side and lower rock cover on the north side. Therefore, most of the radial displacements are inwardly squeezed in the south side, and has an external expansion phenomenon in the north side (Fig. 15 and 16).

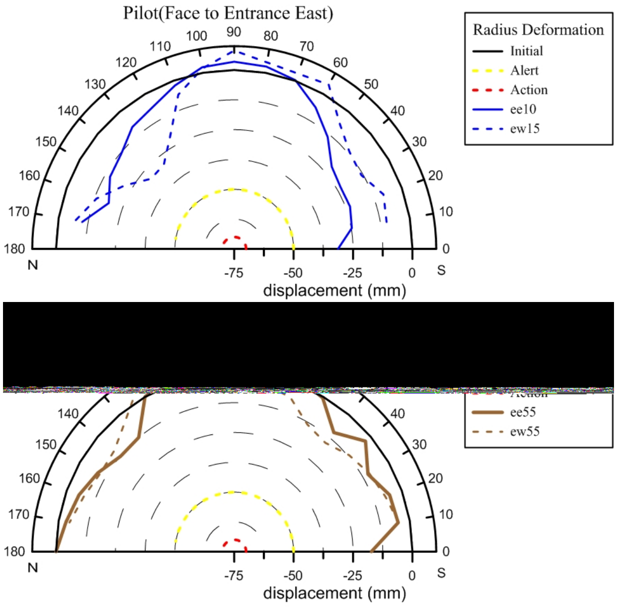

Fig. 13. The radial curve of eastern and western pilot (East, middle, and west).

The displacement of the weakened rock caused by rainfall, which is mainly occurs at the junction between the RC wall and the outer support of the tunnel. The weakest support stiffness is at this junction. From the monitoring results of the radial displacement diagram of the MRT tunnel in Fig. 14, it can be seen that the displacement range is consistent for rainy event. Using 3D LiDAR scanning technology can provide a safety monitoring for adjacent tunnel excavation construction and can have better control in the deformation behavior of rock mass after tunnel excavation. It can maintain tunnel construction safety, and provide reference basis for on-site construction adjustment and design correction.

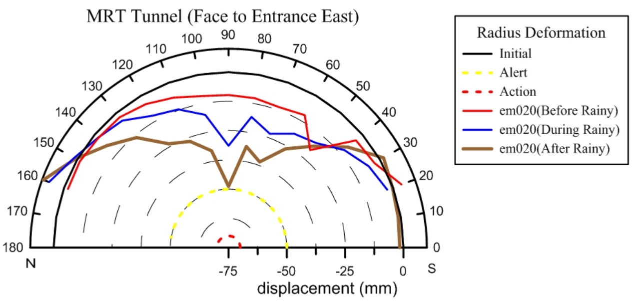

Fig. 14. The radial curve of MRT tunnel (Before and after the rainy season).

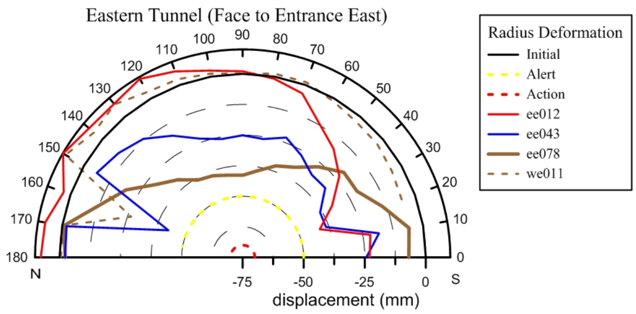

Fig. 15. The radial curve of eastern tunnel (East, middle, and west).

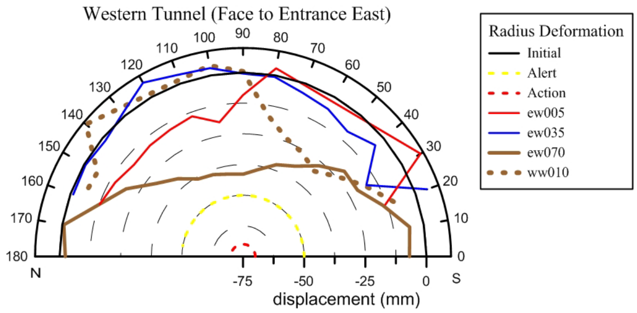

Fig. 16. The radial curve of western tunnel (East, middle, and west).

5 CONCLUSION

This paper highly recommends the use of 3D LiDAR scanning technology for tunnel construction monitoring and tunnel surrounding rock displacement monitoring. It is also applied to multi-arch tunnel, adjacent construction, shallow coverage and the weak strength of the geological rock mass.

Through 3D LiDAR scanning technology, it can quickly obtain high-precision, high-density, and comprehensive three-dimensional spatial coordinate information of tunnels after tunnel excavation.

After the scanning and monitoring data are processed and analyzed, more rock mass displacement around the tunnel can be controlled. For the entire tunnel construction safety monitoring, a complete excavation disturbance behavior mode for surrounding rock can be provided. It can also be applied to more complex excavation disturbances such as special geological structures. The unknown and unpredictable traditional monitoring system for tunnel excavation can be greatly improved, and can be provided more comprehensive monitoring results.

The average displacement is within a range of 25~30 mm for the central pilot (eastern and western pilot) with an average excavation diameter of 6.5 m. The displacement of the surrounding rock of the tunnel is reduced due to the effective application of the central RC wall. After the completion of the double central RC wall, which can effectively inhibit the average displacement of the rock mass to be less than 6mm for the MRT tunnel with an average excavation diameter of 12m.

The weakened rock mass caused by rainy event, resulted in the increment displacement $\Delta\delta_{max}$ of the tunnel rock mass increases by approximately 10~20mm during the rainfall event period. Due to the adjacent construction and shallow coverage factors, the increment displacement $\Delta\delta_{max}$ of the tunnel rock mass also increases approximately 10~20mm

Due to the results of the full-section scanning data of the 3D LiDAR, the overall radial displacement trend is obtained and the displacement contour are provided along the alignment of tunnel. These monitoring results are effective and comprehensive control over the deformation behavior of the surrounding rock of the tunnel, these results can provide a reference for on-site construction adjustment and design correction. If these data combined with more rigorous numerical simulation and feedback design, it is a great help to modern tunnel construction technology.

ACKNOWLEDGEMENTS

During the preparation of this paper, the detailed construction materials and LiDAR monitoring results are provided by the construction contractor Fortune Construction Co., Ltd. These supports are gratefully acknowledged.

REFERENCES

Lemy, F., Yong, S., and Schulz, T., (2006). A case study of monitoring tunnel wall displacement using laser scanning technology. The 10th IAEG International Congress.

Kuo K. J., Tseng H. T., Jhan R. H., and Huang C. H., (2015). The case study for center pillar of triple-arch tunnel, The 14th Cross-Strait Tunnel and Underground Engineering Academic and Technical Seminar. (In Chinese)

Stephanie F., Mark D., and Matthew L., (2010). Geotechnical and operational applications for 3-dimensional laser scanning in drill and blast tunnels, Tunneling and Underground Space Technology, 25(5), 614-628.

Tseng H. T., Kuo K. J., Gao Z. H., and Jhan R. H., (2014). Discussion on the design case of three-arched small clearance tunnel, The 13th Cross-Strait Tunnel and Underground Engineering Academic and Technical Seminar. (In Chinese)

TYLin International Consulting Co., Ltd. (2012). Geological engineering investigation report for design technical services for the second phase of Ankeng Road No. 1 in Xindian District, New Taipei City (Rose Road to Antai Road, and Anho Branch). (In Chinese)

United Geotechnical Engineering Consulting Co., Ltd. (2018). Safety assessment report for the second phase of Ankeng Road No. 1 in Xindian District, New Taipei City (Rose Road to Antai Road). (In Chinese)